X-ray photoelectron diffraction study of perpendicular and tilted CO on clean and potassium-modified Ni(110)

D. A. Wesner,* F. P. Coenen, and H. P. Bonzel
Institut für Grenzflächenforschung und Vakuumphysik, Kernforschungsanlage Jülich, Postfach 1913, D-5170 Jülich, Federal Republic of Germany
(Received 14 November 1988)

The adsorption of CO on clean and K-modified Ni(110) is studied using x-ray photoelectron diffraction at fixed photon energy (Mg $K\alpha$ radiation) to determine precisely the molecular orientation. Enhancements of C 1*s* intensity due to forward scattering from the oxygen atom are measured as a function of polar angle in [001] and [1$\bar{1}$0] azimuths. On clean Ni(110) at 120 K we find a transition from perpendicular to tilted CO with increasing CO coverage. Up to a relative CO coverage of $\sim$0.3 molecules per surface Ni atom, only perpendicular CO is seen. A mixture of tilted and perpendicular CO appears at the coverage $\sim$0.5. At coverages above $\sim$0.9 practically no perpendicular CO remains. In the tilted species, the C—O bond is inclined by 21°$\pm$1° to the surface normal in [001] and [00$\bar{1}$] azimuthal directions, independent of CO coverage. Thermal smearing of the forward-scattering structures due to frustrated molecular rotations decreases for the tilted species because of the tight packing at high CO coverage. The results are qualitatively well reproduced by single-scattering, plane-wave calculations and support a model of island growth of tilted CO domains as coverage increases and crowding and repulsion between adjacent molecules sets in. Perpendicular and tilted CO were also observed on K-covered Ni(110) but at lower CO coverages and at 300 K. A much different process causes tilting of CO molecules in this case. Potassium precoverages of as little as 0.08 induce tilting of some of the molecules in the [001] and [00$\bar{1}$] directions, with the fraction of tilted CO growing with K precoverage. Some dependence of tilt angle on K coverage is evident: up to 0.34 an angle of 32° to the surface normal and above this coverage about 27°. This change in tilt angle is accompanied by a reduction of the CO sticking coefficient. No evidence for adsorption of CO atop K adatoms is seen. Potassium-affected, tilted CO is more strongly adsorbed relative to perpendicular CO and has a reduced thermal smearing of forward-scattering structure. These data and previous results on this system suggest a strong, short-range K-CO interaction with the tilted CO adsorbed near K adatoms in the atomic troughs between rows on the (110) surface. The tilted CO on clean Ni(110) at 120 K and that on K-precovered Ni(110) at 300 K thus have a similar orientation, but there are quite different physical origins for the tilt.

I. INTRODUCTION

The two-dimensional symmetry of an adsorbate layer is relatively easy to determine, e.g., via low-energy electron diffraction (LEED). Methods to measure the *microscopic* structure of an adsorbate layer, such as the orientation of a molecular axis relative to the surface, are much less common. Such information can be won from complete LEED structure determinations or by the analysis of surface-extended x-ray-absorption fine-structure measurements (SEXAFS). Both are relatively involved and "indirect," i.e., model calculations must be done and the results compared to experiment in order to decide on a structure. High-resolution electron-energy-loss spectroscopy (HREELS) is also used in a "fingerprinting" mode to draw indirect conclusions about adsorbate structure. A given value of a vibrational loss is associated with a certain bonding geometry, either from measurements on standard, known systems or from comparison to calculations. Several types of photoemission symmetry measurements can be used to determine adsorbate geometry. These include the dependence of the photoemission signals from molecular orbitals[1] or from structures in the near-edge x-ray-absorption fine structure[2] (NEXAFS) on experimental parameters such as photoelectron emission angle or photon polarization. These methods are more or less direct, but can have a relatively weak dependence on changes in bond angles, so that a molecular orientation may often be determined only to an accuracy of $\pm$5°.

A fundamentally different method uses photoelectron diffraction in the final state.[3,4] This can be done at low or high photoelectron kinetic energies, but for high enough kinetic energies (>200 eV) the scattering becomes relatively simple. Almost all the scattering occurs in a narrow (10°–20°) cone in the forward direction (scattering angle 0°), in what has been called a "forward focusing" process. Multiple scattering effects are much reduced in comparison to scattering at LEED energies, where the scattered intensity is distributed over a much larger angular range.[5] Therefore, information on adsorbate orientation can be more or less directly read from the experimental intensity patterns. The data are not associated so much with diffraction, i.e., representing a Fourier transform of a surface structure, but are rather an image of

real space axes. In spite of this the method has become known as x-ray photoelectron diffraction (XPD); a more descriptive name might be x-ray photoelectron forward scattering. In the type of information obtained for adsorbates, XPD closely resembles the technique of measuring electron-stimulated-desorption ion angular distributions (ESDIAD). In ESDIAD one detects the energetic ions emitted when an electronically excited adsorbate molecule dissociates (e.g., O^+ from adsorbed CO). Trajectories of such ions are directed primarily along the molecular axis, so that the measured ion angular distribution reflects the adsorbate orientation.[6] More will be said about similarities and differences between ESDIAD and XPD below.

We have recently completed an extensive study of the adsorption geometry of CO on clean and K-covered Ni(110) by XPD. This paper presents the complete report of that study; preliminary results were already published elsewhere.[7,8] It has two sections: CO adsorption at low temperature on clean Ni(110), and room-temperature adsorption of CO on surfaces with submonolayer K precoverages. The former case has been well studied by other surface-science techniques, and we obtain results in general agreement with these earlier studies. Much less is known about the latter system, CO+K on Ni(110). Our goal here was to look for alkali-metal-induced changes in CO orientation, such as have been suggested in other systems. We begin below with a description of the experimental apparatus and procedures, followed by results and discussions of the two adsorption systems.

II. EXPERIMENTAL APPARATUS AND PROCEDURES

An ion-pumped ultrahigh vacuum (UHV) chamber having a base pressure of about 3×10^{-11} mbar and facilities for Auger electron (AES) and x-ray photoemission (XPS) spectroscopies, as well as for sample preparation, was used for all the work described here. The Ni(110) single crystal was cleaned *in situ* by standard sputter-anneal cycles until no impurities could be detected by AES or XPS. During measurements the sample was either at room temperature or cooled to about 120 K by liquid nitrogen. CO exposure was done by backfilling the chamber to a pressure in the 10^{-8}-mbar range. Exposure values based on the (uncorrected) ion gauge pressure and dosing time are given below in Langmuirs (L, 1 $L=1.33\times10^{-6}$ mbar s). These must be considered approximate ($\pm\sim20\%$) because of uncertainty in the ion gauge calibration. Potassium was deposited by evaporation from a thoroughly degassed commercial dispenser source (SAES Getters, GmbH). The amount was calculated from the K(*LMM*) to Ni(L_3VV) AES peak ratio, assuming this to vary linearly with coverage in the submonolayer range. As a calibration point, room temperature saturation was taken to be a relative coverage $\Theta_K=0.53$ K atoms per Ni surface atom (i.e., 6.04×10^{14} K-atoms/cm^2).[9] Coadsorption was always done by exposing a K-precovered surface to CO.

As described previously,[10] the apparatus allows for variation of the photoelectron polar angle $\theta\pm60°$ from the surface normal ($\theta=0°$) by rotation of the sample about a horizontal axis lying in its surface. Thereby the angle-resolving hemispherical electron energy analyzer (Leybold EA-10, 100 mm radius) and the Mg anode x-ray source (photon energy 1253.6 eV) remain fixed. The former has a vertical acceptance axis, while the latter is aligned so that x rays are incident at 60° to the analyzer acceptance axis, in the plane defined by this axis and the sample rotation axis. This arrangement produces symmetric x-ray illumination of the sample. The photoelectron azimuthal angle is fixed for a particular sample installation. We used two azimuths, the detected photoelectron parallel momentum being either in the [001] crystal direction (i.e., the sample is rotated about an axis parallel to the $[1\bar{1}0]$ direction), or 90° away in the $[1\bar{1}0]$ direction (sample rotation axis parallel to [001]).

The core-level intensity is measured by counting at three kinetic energies: the peak and two background energies on either side and well removed ($\sim\pm3$ eV) from it. A linear extrapolation between the two backgrounds yields the value to be subtracted from the peak count rate to give the net peak height. It was checked earlier[10] that this procedure yielded the same results as the more time-consuming method of integrating a complete core-level spectrum and subtracting an extrapolated background. Measurements were usually made at relatively poor analyzer resolution (~1.5 eV), both to smear possible line-shape structure as well as to increase the count rate. The peak height measurement is repeated in 1° steps over the 120° polar-angle range (θ precision $\pm0.5°$). Automation of the θ rotation allowed convenient multiple scanning ($\sim10\times$) instead of once-through scans, which averages out slow x-ray intensity variations. The time for a spectrum varied depending on adsorbate coverage; an average run took about 4–5 h. In spite of the relatively good vacuum, for such long counting times we were concerned about possible surface contamination, and the surface was periodically checked with XPS scans.

For high photoelectron kinetic energies (i.e., for C 1*s*, ~964 eV; for K $2p_{3/2}$, ~956 eV; and for O 1*s*, ~717 eV), we expect the angular dependence of core level intensity to be dominated by forward-scattering structure from nearby neighbors. If the geometry is such that these are *not* observable, then the only contribution to structure will be from slowly varying factors which can be termed the "instrumental response."[3] An example would be the K 2*p* signal from a single K layer on a transition metal. Because of repulsion between the partially ionic adatoms, most alkali metals adsorb in a single layer with little tendency to second-layer growth before first-layer saturation is reached.[11] Angular intensity distributions from such a situation are shown in Fig. 1. Potassium 2*p* intensities (both $\frac{3}{2}$ and $\frac{1}{2}$ levels exhibit the same structure) for coverages near first-layer saturation in both azimuths are plotted. Here and in following figures both the data points and a smoothed line obtained by a Fourier transform smoothing routine are shown. One instrumental factor has already been included: the net peak height at each θ has been multiplied by $\cos(\theta)$ to compensate the intensity increase from the larger sampled area (growth of the projected entrance slit on the sample) at large θ. An intensi-

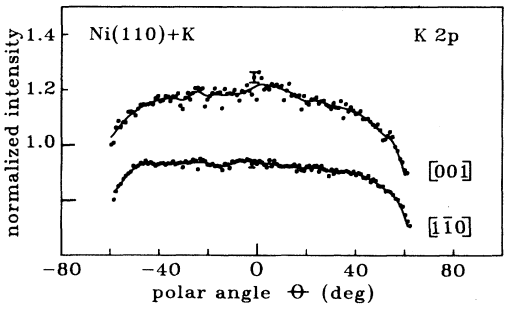

FIG. 1. XPD scans of K 2*p* intensity from submonolayer K coverages on Ni(110) at 300 K. The coverage is 0.53 for the [001] azimuth and 0.42 for the [110] azimuth. The ordinate pertains to the [001] azimuth; the [1$\bar{1}$0] azimuth scan is shifted downward. In this figure and in those following, a typical error bar, based on statistical counting noise, is shown near $\theta=0°$.

ty normalization to 1.0 at $\theta=-60°$ has also been done to facilitate the comparison between curves of varying intensity. What remains is a structureless θ dependence up to about $\theta=\pm 50°$, where a slow decrease of intensity sets in. Around this angle the projected entrance slit is actually wider than the sample, so that intensity is lost. An underlying structure similar to that in Fig. 1 is thus to be expected in all our measurements, and we correct for it below by dividing through by a suitably normalized curve like those in Fig. 1. The only remaining θ variation (barring multiple-scattering effects) then comes from forward-scattering enhancements.

III. CO ON CLEAN Ni(110)

A. Previous work

Studies of CO adsorption on clean Ni(110) have been made using a wide range of surface-science techniques. Early LEED work identified several superstructures depending on CO coverage.[12] In particular, at a high relative coverage of 0.9–1.0 CO molecules per surface Ni atom a 2×1 pattern is observed which can be ascribed to a structure having *p2mg* symmetry. To achieve the high coverage associated with this layer it is necessary to cool the sample to less than about 250 K, or, if exposing at 300 K, to measure in a CO ambient atmosphere. The room-temperature saturation coverage for a nonambient exposure is about 0.7,[13] and a clear 2×1 structure is not observed. A detailed LEED study[14] of adsorption at 130 K measured the intensities of various superstructure beams as coverage was increased to $\theta=1.0$. The 2×1 LEED spots coexist with those of other structures beginning at coverages as low as about 0.40. Their intensity increases with CO coverage until, at a coverage of about 0.95, only the 2×1 pattern remains. The authors interpret the LEED data as consistent with an island growth mechanism of the 2×1 phase.

Other experiments have probed the local structure of the adsorption site. High-resolution electron-energy-loss (HREELS) measurements of the C-O stretch frequency have found values appropriate for perpendicularly adsorbed CO over most of the CO coverage range.[13,15] On-top and short-bridge adsorption sites on the atomic rows along the [1$\bar{1}$0] direction coexist in roughly the same intensity ratio at all coverages up to about 0.8. Beyond this point (at coverages corresponding to the 2×1 phase) the on-top and bridge losses merge into a single loss peak. While little speculation about the structure of this phase came from HREELS studies, one group did interpret the reduced loss intensity of the 2×1 phase as consistent with a tilt of the C—O axis by at most 55° to the surface normal.[15] The (2×1) phase has also been studied with angle-resolved photoemission[16] (ARUPS) and with ESDIAD.[17,18] Symmetry considerations applied to the ARUPS data showed that in the 2×1 phase the C—O bond tilts 17° from the surface normal along the [001] direction. This was more directly seen in the ESDIAD results in which a tilt angle of 19° to the surface normal, again confined to the [001] azimuth, was observed. ESDIAD profiles taken in this azimuth show a single lobe representing the C—O bond directed along the normal for CO coverages less than about 0.66.[17] At coverages above 0.82 a clear double-peak structure appears. The results imply a coverage-independent tilt angle for the high-coverage phase and its growth via island formation. A theoretical understanding of the origin of this tilted phase had been already given by Bauschlicher,[19] who showed in model calculations that the repulsion between O ends of adjacent CO molecules adsorbed on the atomic rows of a fcc (110) surface can be significantly reduced by allowing the perpendicularly adsorbed molecules to tilt away from normal. For Ni(110) the calculated minimum-energy configuration usually involved a polar-angle tilt of about 20°–35°. Tilts in various azimuths were also tried, but no calculationally significant differences were seen. A tilting into the "valleys" between [110] atomic rows is intuitively reasonable. The double periodicity of the 2×1 structure arises through alternation of the tilt direction between [001] and [00$\bar{1}$] along the rows.

B. Results and discussion

Figures 2 and 3 show our results in the [001] and [1$\bar{1}$0] azimuths, respectively, for the C 1*s* level of CO adsorbed at 120 K on Ni(110). As discussed above, the data have been corrected for instrumental response by dividing by a normalized K 2*p* intensity distribution from a submonolayer K coverage. In each figure we show results for several CO exposures. The curves do not all have the same signal-to-noise relation because measuring times were not the same for each.

Consider first the data for the [001] azimuth in Fig. 2. At the lowest CO exposure of 0.5 L a peak centered along the surface normal appears with a maximum intensity about 40% larger than at the $\theta=-60°$ normalization point. We interpret this as the forward-scattering enhancement of C 1*s* intensity due to scattering from the oxygen atom in perpendicularly adsorbed CO. The amount of enhancement is reasonable in comparison to previous XPD results for perpendicularly adsorbed CO

on other surfaces.[4,10,20–22] However, the peak full width at half maximum (FWHM) of 28° is larger than the "natural" linewidth of about 22° as obtained from plane-wave, single-scattering calculations (SSC's) using atomic scattering factors.[10,23] In calculating the FWHM we use the minimum value of intensity (e.g., near $\theta=\pm 30°$ in the 0.5-L scan of Fig. 2) as background. Because of the noise level in some scans this cannot always be well defined; we estimate an error of about $\pm 1°$ on the FWHM values. Conceivably, the peak broadening could arise from a nonzero polar tilt angle in the adsorbed CO layer. Assuming a complete azimuthal freedom for the tilted C-O axis, a polar tilt of about 5° would then explain the observed peak FWHM. A second possibility is that the CO is oriented on average in the normal direction, but that the molecule undergoes a thermal "wagging" vibration (i.e., a frustrated translation[24]). The photoemission

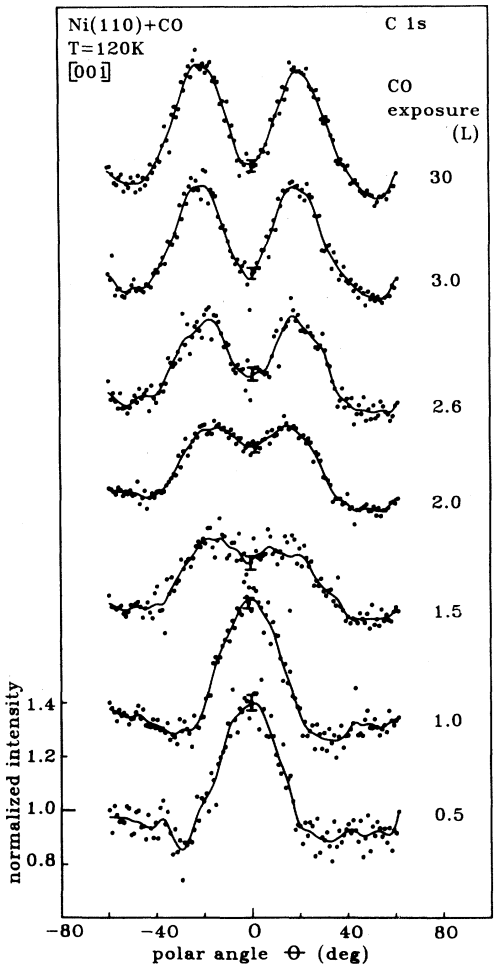

FIG. 2. XPD scans of C 1*s* intensity in the [001] azimuth for CO adsorbed at 120 K on clean Ni(110), normalized to remove the instrumental response (see text). The CO exposure in L for each scan is indicated. The ordinate pertains to the 0.5-L scan; the others are shifted upward.

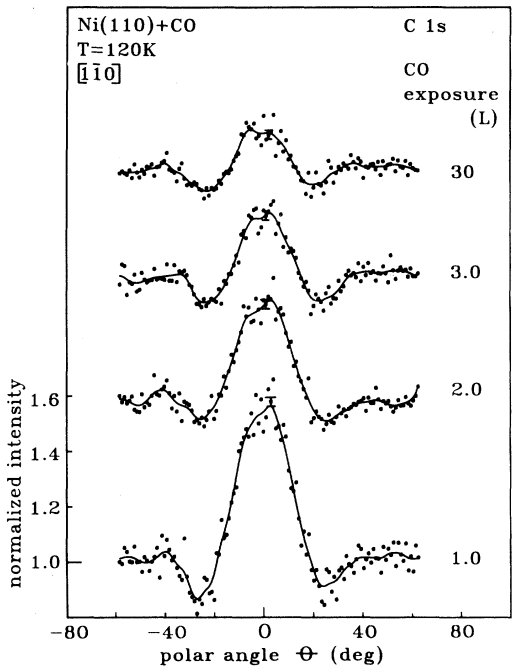

FIG. 3. Similar to Fig. 2, for the [1$\bar{1}$0] azimuth.

occurs on a much shorter time scale than this vibration and thus averages over an ensemble of molecular orientations. Such an ensemble averaging can be incorporated in the SSC, yielding smeared forward-scattering structure.[23] As discussed in more detail elsewhere,[8] we believe this latter explanation to be correct. Briefly, the peak width is strongly temperature dependent (cf. Figs. 2, 3, 5, and 6 below), as would be expected for a vibrational effect. At a given temperature there are also differing peak widths between [001] and [110] azimuths (cf. Figs. 2 and 3) that are consistent with an anisotropic restoring force for the vibrations in the asymmetric adsorption sites atop atomic rows on the (110) surface.

As the CO exposure is increased to 1.0 L in Fig. 2, no significant changes in the peak width or intensity occur. Using the coverage-versus-exposure relations obtained by Behm *et al.* from thermal desorption (TDS) measurements,[14] the coverage is about 0.15 and 0.3 for exposures of 0.5 and 1.0 L, respectively. In this range no tilted CO is observed, in good agreement with the LEED results.[14] At 1.5 L (coverage ~ 0.5) a large change is observed. The main peak is about twice as wide as before. Detailed structure in this peak is not visible: Appreciable intensity appears at all angles from about $-35°$ to $+35°$. (Partly this is due to a lower signal-to-noise ratio is this scan.) A similar distribution exists after a 2.0-L exposure (coverage ~ 0.6), but here a double-peak structure with intensity lobes at $\theta=\pm 21°$ begins to appear. There is still appreciable intensity at $\theta=0°$. The same can be said for the 2.6-L exposure (coverage ~ 0.8); the $\pm 21°$ peaks become more pronounced in relation to the intensity at $\theta=0°$. In this coverage range several different LEED patterns coexist.[14] Saturation appears to have been reached at 3 L

(coverage ~ 0.9), because little changes between this scan and that after 30-L exposure (coverage $=1.0$). The peaks at $\pm 21°$ are well defined and virtually no enhancement remains at $\theta=0°$ corresponding to perpendicular CO. From these data we conclude that at saturation there is a homogeneous layer present in which the C-O axis assumes a mean tilt angle of $21°\pm 1°$ from normal in the [001] and [00$\bar{1}$] directions. The 30-L data in Fig. 2 have a sufficiently good signal-to-noise ratio that we could probably even distinguish changes of less than 1° in the mean tilt angle. The thermal broadening of the peak observed at low coverage has even become smaller: The FWHM for one of the 21° lobes at 30-L exposure is 23°, compared to 28° for the single peak at 0.5 L. This is reasonable, since we know the 2×1 layer has a very dense CO packing. The frustrated translational motion which is responsible for the peak broadening must be even more frustrated at high coverages due to steric constraints.

A tilt in azimuthal directions other than [001] is unlikely. In that case, such strong forward-scattering enhancement as seen in the 30-L spectrum of Fig. 2 would not be obtained for the [001] azimuth: Intensity would be distributed in other directions. Exactly such an effect was suspected for the 2×1 CO adsorption system on Pt(110).[22]

It also appears that the transition from perpendicular to tilted CO proceeds via growth of islands having tilted CO at the expense of those with perpendicular CO. The presence of a mixture of tilted and perpendicular CO is evident in all the intermediate exposure data (1.5, 2.0, 2.6 L) in Fig. 2. We can, in fact, reproduce the shape of each of these curves very well by taking various linear combinations of the 0.5- and 30-L curves. (Roughly, the data for 1.5, 2.0, and 2.6 L correspond to about 40%, 60%, and 80% tilted CO, respectively.) If the transition to tilted CO involved, e.g., a monophase layer with a single, CO-coverage-dependent value of the tilt, this would not be possible and a more continuous broadening of the forward scattering peaks would be expected with increasing coverage.

The [1$\bar{1}$0] azimuth data in Fig. 3 support this general interpretation. In this azimuth we should observe mainly perpendicular CO because tilted CO is directed 21° out of the measuring plane. At 1.0-L exposure we find perpendicular CO with a forward-scattering peak FWHM of 25° arising from the smaller vibrational broadening in this azimuth.[8] With the resultant improved angular resolution there are hints of secondary maxima at about $\pm 40°$ situated from the main peak. These are correctly positioned to be the first-order diffractions predicted by SSC's (Refs. 10 and 23) corresponding to the interference between a C 1*s* photoelectron wave coming directly from the C atom and one which has been scattered from the O atom. The path length difference between these causes a phase difference which, together with the intrinsic scattering phase change, produces constructive interference near 40° (and destructive interference near 25°). Because the scattering from the O atom is so forward peaked, these diffraction peaks are relatively weak and easily obscured by vibrational broadening. As CO coverage is increased, less and less intensity is seen at $\theta=0°$, corresponding to the gradual disappearance of perpendicular CO. Strangely, the first-order diffraction structures remain at all coverages. This is due to a fortuitous feature of this adsorption and measurement geometry. The diffractions are, of course, positioned cylindrically symmetric about the C—O bond axis for either perpendicular or tilted molecules. It so happens that even for tilted CO they are visible in this azimuth at about the same sample polar angle ($\theta\sim 35°$) as for perpendicular CO.

The small peak remaining at 0° for 30 L, i.e., saturation coverage, is not a remnant of perpendicular CO: This would be incompatible with the observed low intensity at $\theta=0°$ in the [001] azimuth (Fig. 2). It has its explanation in the detector geometry. The acceptance area of the detector is an image of the 2×10-mm^2 entrance slit projected onto the surface by the electron optics. The long axis of this slit image is parallel to the sample (θ) rotation axis. This orientation causes an intrinsically larger detector angular acceptance in the direction parallel to the sample rotation axis as in that perpendicular to it. For the CO molecules that are tilted in the [001] azimuth and observed in the [1$\bar{1}$0] azimuth there is thus an effectively larger angular acceptance. The peak at 0° in the 30-L spectrum then simply arises from the tails of forward-scattering cones of tilted CO.

The picture which emerges from the XPD data generally supports the conclusions of LEED (Ref. 14) and ESDIAD (Refs. 17 and 18) studies. There is, however, a small disagreement between these studies. LEED shows a mixture of the 2×1 tilted species coexisting with other surface species already at a CO coverage of ~ 0.40. ESDIAD results show a single O^+ emission lobe directed along the normal, presumably corresponding to perpendicular CO, even at coverages as high as 0.66 (Ref. 17) or 0.75 (Ref. 18). A splitting of this structure occurs only above this coverage range. Our results are thus more in agreement with the LEED study. One possible difficulty in comparing the XPD and LEED data with ESDIAD is that in the latter case there is a coverage-dependent positive ion yield. This is due to intermolecular quenching effects in the desorption process[17] and, conceivably, could lead to different excitation probabilities for tilted and perpendicular CO. In XPD no such coverage-dependent cross-section effects are expected.

C. Comparison to calculations

Plane-wave, single-scattering calculations were done in order to confirm our interpretation of these experimental results. The method, similar to that of Fadley and Thompson,[23] uses tabulated atomic scattering amplitudes and phases.[25] Vibrations are taken into account by allowing the C—O bond direction to vary isotropically and randomly from its mean orientation. For each random molecular orientation the XPD angular distribution is calculated. A large number ($\sim 10\,000$) of such curves, suitably normalized, are summed to yield the final result. The normalization factor for a given vibration is

$$P(\theta_v)=\exp(-\theta_v^2/2\theta_{\rm rms}^2)d\Omega\ ,$$

where θ_v is the polar vibrational angle relative to the

mean C—O bond direction, θ_{rms} is the root-mean-square vibrational angle (a parameter in the calculation), and $d\Omega$ is a solid angle element at θ_v. Complete freedom is allowed for the azimuthal orientation of the vibration about the mean direction. The results for both azimuths are in Fig. 4. Vibrational averaging was done with $\theta_{rms}=8°$. This value gave the best fit to the observed peak FWHM. Similarly to the experimental data, a normalization to 1.0 at $\theta=-60°$ has been made, as well as a smoothing with an averaging window 8° wide, to try to account for the nonzero analyzer angular acceptance. No attempt was made to include the nonisotropic detector angular acceptance discussed above. When the calculated curve for the [001] azimuth is suitably scaled down in intensity by a factor of 2.5 (note the ordinate in Fig. 4), the agreement with the experimental curve at the top of Fig. 2 is very good. The scaled theoretical and experimental angular distributions have essentially the same shape, even including such details as the minima in intensity at about ±50°, presumably due to the destructive interference effect discussed above. This agreement gives us further confidence in the structure determination. The quantitative disagreement is not so serious, since plane-wave calculations are known to overestimate the forward-scattering intensity enhancement. Previous studies of this effect for scattering from Ni at 950 eV (Ref. 26) have found that decreases in intensity by factors of ~2 can be expected in the forward direction when a more exact spherical-wave calculation is made. The overall shape of the curves remains unchanged, however, showing that the plane-wave approach is an appropriate approximation. In the [1$\bar{1}$0] azimuth the agreement with experiment is not as good. The explanation for the high intensity at $\theta=0°$ was given above, but the measured first-order diffraction structures near ±40° are also ostensibly too strong: about as intense as predicted from the plane-wave calculation. The explanation lies in the *angular* dependence of the calculated plane-wave versus spherical-wave intensity difference. At least for scattering from Ni at 950 eV, this difference goes down with increasing scattering angle and is essentially negligible above about 50° scattering angle.[26] Since we believe the structures at ±40° in our data for [1$\bar{1}$0] are due to large-angle scattering and not to forward scattering, it is thus reasonable to expect a somewhat better agreement with the intensity predicted for them by the plane-wave calculation.

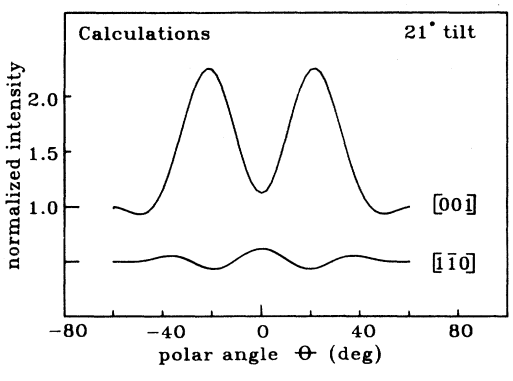

FIG. 4. Single-scattering plane-wave calculations in both measurement azimuths for the C 1*s* XPS intensity for a model having CO tilted ±21° in the [001] azimuth. The ordinate pertains to [001].

IV. COADSORPTION OF CO AND K ON Ni(110)

A. Previous work

There are numerous studies of CO plus alkali-metal coadsorption systems using many surface-science techniques.[11] One aspect of the alkali-metal–CO interaction that has received particular attention is the possibility of alkali-metal-induced tilting of the molecular axis from its "normal" perpendicular orientation. A molecule with a substantial polar-angle tilt or lying flat on the surface would probably have some of the characteristics of alkali-metal-affected CO seen in the surface-science experiments. For example, a weakened C—O bond and a shifted C-O stretch frequency might result from the increased occupation of the antibonding CO 2π molecular orbital expected in a side-on bonding configuration.[27] Such an explanation was proposed for CO and K coadsorption at 80 K on Ru(001).[28] At low coverages (~0.10) for K and CO an extremely low C-O stretch frequency (1400 cm^{-1}) is observed, which, together with other observations, was taken as evidence of a side-on bonded molecule. ESDIAD measurements on this same system by other investigators[29] showed that the O^+ ion signal from perpendicularly adsorbed CO is systematically reduced with increasing K coverage in the range up to $\Theta_K=0.15$. This is consistent with a molecule so strongly tilted that the emitted O^+ ion is reneutralized before it can be detected. This requires a polar-angle tilt of more than about 60°. Alternatively, it can be explained by an increased ion neutralization rate for perpendicular molecules in the presence of the alkali metal, which decreases the ESDIAD yield. A similar effect was seen for CO+K on Ni(111).[30] In contrast, angle-resolved photoemission measurements of the CO valence levels with synchrotron radiation have been used to place an upper limit of 30° on the CO tilt angle for the low-coverage coadsorption layer (and for higher CO and K coverages as well).[31] Similar conclusions are reached for the CO on Cu(100)+K coadsorption system.[32] The existence of perpendicular CO for the higher K and CO coverages has also been seen in x-ray-excited, angle-resolved AES measurements,[33] in which the polar-angle dependence of various Auger structures is only compatible with a molecule tilted at most 5° from normal. While the case for tilted CO on Ru(001)+K is thus controversial, ESDIAD measurements on the presumably similar coadsorption system of CO+Na on Ru(001) have given direct evidence for tilted CO.[34] In this case the O^+ ESDIAD pattern from CO does not disappear upon alkali-metal coadsorption, but rather a hexagonally segmented halo appears with lobes of intensity oriented 50° to the surface normal. The corresponding CO tilt is probably less than 50° because of

the image-potential effect on the ESDIAD ion trajectories. The authors conclude that CO is adsorbed on the Ru surface near a Na adatom and probably tilts toward it because of an interaction of the O end of the molecule with the slightly positive Na. One aspect, however, is puzzling. The halo pattern appears only at low relative Na coverages (up to 0.15) and high CO coverages. It is also extremely temperature dependent, disappearing above 90 K. Otherwise perpendicularly adsorbed CO is seen. The low thermal stability of this Na-induced CO structure is unusual because normally alkali metals tend to increase the adsorption energy of CO and thus stabilize corresponding CO structures.

Other surfaces on which strong changes in CO adsorption geometry induced by K coadsorption were suspected include Cu(110) and Ni(111). In the former, HREELS and TDS measurements were interpreted in terms of the formation of a surface compound similar to a K salt, chiefly on the strength of comparisons to measurements on model compounds.[35] In the latter, changes in the metastable quenching spectra (MQS) of low kinetic energy, excited He atoms scattered from the surface were studied[36] and interpreted in terms of a transition to a flat-lying or strongly tilted CO molecule with increasing temperature. Against these indirect indications of tilted CO stand direct measurements of perpendicular CO on Pt(111) with coadsorbed Na or K. The photon-polarization dependence of NEXAFS for saturation CO coadsorbed with Na showed that the CO polar tilt angle is smaller than about 15°, while the C—O bond length increases by 0.12 Å, due to the interaction with the alkali metal.[37] In the case of Pt(111)+K, XPD measurements in our laboratory have shown that CO is perpendicularly adsorbed both on the clean surface and in the presence of K for a wide range of K and CO coverages.[10,38] This occurs in a system in which a strong, short-range K-CO interaction is seen in HREELS, with C-O stretch frequencies as low as 1390–1420 cm^{-1}.[38,39] From these few examples it is clear that the question of alkali-metal-induced CO orientation changes remains unsettled.

To shed light on this problem, we studied the coadsorption of CO and K on Ni(110). One might expect this fcc (110) surface to be a good candidate for observing tilted CO in the presence of an alkali metal. The adsorption sites for K are thought to be the valleys between $[1\bar{1}0]$ atomic rows,[9] while CO adsorbs in on-top and short-bridge sites atop the rows. This situation represents an inherently lower symmetry than on, e.g., a fcc (111) or hcp (001) surface on which one might expect three or six possible symmetry-equivalent CO adsorption sites near an adsorbed alkali-metal adatom. We also have the already known example of a tilted CO species on this surface, albeit at low temperature and having a much different physical cause. Further, Whitman and Ho, who studied this system with TDS, LEED, and HREELS,[40] find an unusually distinct coexistence of K-affected and -unaffected CO as compared to other coadsorption systems. The most strongly K-affected CO species can even be isolated on the surface by thermal desorption of less strongly bound species, which makes identification of adsorption geometry easier than on a surface on which several species coexist, e.g., Cu(100).[41] Whitman and Ho found that after heating a coadsorbate layer (K precoverage 0.13) to 485 K, only strongly affected CO, which they designated CO*, was observed, having a C-O stretch frequency of 1660 cm^{-1}. From their LEED observations they also conclude that this heating causes diffusion of the coadsorbates both over and along the troughs in the $[1\bar{1}0]$ direction, resulting in a contraction of the K and CO into islands with local K coverage 0.25 and with roughly two CO* molecules coordinated to each K. They proposed that CO* is adsorbed in a displaced bridge site atop the $[1\bar{1}0]$ atomic row and directly adjacent to a K adatom adsorbed in a fourfold hollow site in the trough between rows.

B. Results and discussion

Our XPD data for CO+K coadsorption were all taken at room temperature (300 K). CO exposure was usually 3 L for K coverages up to about $\Theta_K=0.35$. This was sufficient to reach the saturation CO coverage of about 0.7 for surfaces without K. Whitman and Ho find from TDS measurements that the saturation CO coverage decreases to 0.50 at $\Theta_K=0.20$. We estimate from XPS intensities that the saturation CO coverage remains approximately constant between $\Theta_K=0.20$ and 0.53 (the saturation K coverage), but find a drastically reduced CO sticking coefficient for K coverages greater than about $\Theta_K=0.35$. Above this level we exposed to 30 L CO before measurements in order to get saturation CO coverage. For all the coadsorbate layers studied the C and O 1*s* XPS line shapes gave no evidence for dissociated CO. This would be especially evident in the C 1*s* line shape, which would show an extra peak for dissociated, carbidic C at around 283 eV binding energy, well separated from the molecular peak near 285.7 eV.[42,43] Both C 1*s* and O 1*s* peaks shift to lower binding energies with increasing K coverage, similar to XPS results in other systems[43,44] and consistent with K-induced charge transfer to the molecule.

We plot in Figs. 5 and 6 C 1*s* XPD angular distributions in the [001] and $[1\bar{1}0]$ azimuths, respectively, after a 3-L CO exposure to surfaces with various K precoverages. The lower curve of each figure is the clean-surface result; virtually identical results are obtained after 1.5 or 30-L CO exposures. A single peak centered along the surface normal appears in both azimuths. Both clean-surface curves are considerably broader at 300 K than that of perpendicularly adsorbed CO at 120 K (Figs. 2 and 3). The asymmetry between azimuths due to the asymmetric vibrational amplitude appears here also.[8] Similar to the low-temperature results, we interpret these data in terms of perpendicularly adsorbed CO with thermal smearing of the forward-scattering structure. With adsorbed K the angular distributions change dramatically. A double-peak structure corresponding to tilted CO appears in the [001] azimuth with peaks near ±32°. Although this angle is larger than the ±21° observed for the high-coverage CO layer on clean Ni(110) at 120 K, the minimum between the peaks is not so well defined as in the top curve of Fig. 2. This suggests that a

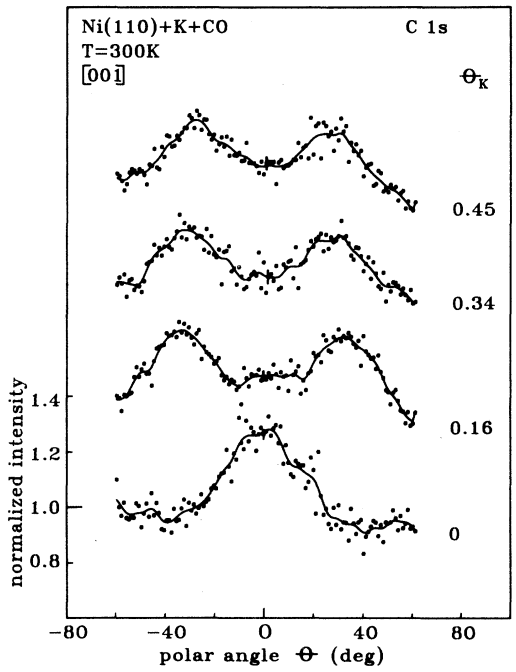

FIG. 5. Normalized XPD scans in the [001] azimuth for the C 1s intensity from CO adsorbed on a Ni(110) surface at 300 K with various K precoverages. The K coverage is indicated for each scan. The CO exposures were 3 L for each scan except for K coverage 0.45, in which case the exposure was 30 L.

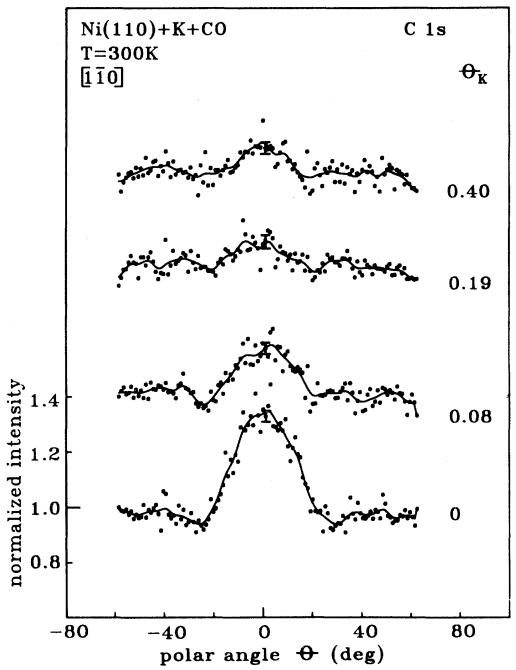

FIG. 6. Similar to Fig. 5, for the [1$\bar{1}$0] azimuth. The CO exposures were 3 L for each scan except for K coverage 0.40, in which case it was 30 L.

remnant of vertically adsorbed CO is still present. Such a suspicion is confirmed by the [1$\bar{1}$0] azimuth data in Fig. 6, where no tilted CO is visible, but only a peak centered at 0°. This peak is not due to the tails of the forward-scattering cones of tilted CO and the larger angular resolution parallel to the entrance slit, as was the case for the clean-surface data of Fig. 3; the larger tilt angle for K-affected CO should minimize the effect discussed above. We conclude that this peak represents perpendicular CO, a conclusion which is confirmed by the behavior of the peak after surface heating (to be discussed below). The amount of perpendicular CO goes down with increasing K coverage, decreasing the observed forward-scattering peak. Some, however, is present even at a coverage $\Theta_K=0.40$. In the [001] azimuth ±32° tilted CO mixed with perpendicular CO is seen for $\Theta_K=0.16$ and 0.34, but at $\Theta_K=0.45$ a subtle change occurs. The forward-scattering peaks move inward to about ±27°. This K coverage is above the value at which the drastically reduced CO sticking coefficient sets in, and it is possible that a different bonding configuration exists in this K-coverage range. However, it in any case still involves a mixture of tilted and perpendicular molecules.

Comparing the peak FWHM in the [001] azimuth as a function of K coverage, we find that the lobes for tilted CO are significantly narrower (~25°–30° FWHM) than that of perpendicular CO on the clean surface (~38° FWHM). The forward-scattering lobes of tilted CO are less thermally broadened, probably because of the strong interaction with K, which is known to stabilize the molecule. Interestingly, a related effect was recently observed in ESDIAD for the interaction of CO with Se on Pt(111).[45] Although the CO-Se interaction is repulsive, it nevertheless reduces vibrational broadening of the CO ESDIAD pattern, compared to CO adsorbed alone, similar to the effect of K on the CO XPD angular distributions. In the case of the high-symmetry Pt(111) surface, the CO adsorption sites are symmetrically surrounded by repulsive Se adsorbate atoms, and the interaction decreases the amplitude of the frustrated rotation. In contrast to the peak narrowing observed for K-affected, tilted CO on Ni(110), the lobes at $\theta=0°$ in the [1$\bar{1}$0] azimuth for various K coverages have about the same FWHM for clean and K-covered surfaces, within the signal-to-noise constraints of the data. This is because they result from perpendicular CO molecules adsorbed on relatively "clean" areas of the surface not near a K adatom. The O 1s levels from CO adsorbed with various K precoverages showed no structure attributable to forward-scattering. Likewise, the K $2p_{3/2}$ peaks showed no change in their angular dependence due to CO coadsorption, remaining relatively structureless, as in Fig. 1. We can thus rule out adsorption modes involving the CO molecule adsorbed atop K adatoms. A totally flat-lying molecule is also impossible, since then neither the C 1s nor the O 1s level would have forward-scattering enhancements. Based on the known, short-range nature of the CO–alkali-metal interaction in several systems,[38,39,46] we believe that the tilted CO molecules are adsorbed very near the K, but still coordinated to the metal surface.

A close interaction between the tilted CO and K is im-

plied by the data in Fig. 7. Here we show C 1*s* XPD angular distributions in both azimuths from a coadsorbate layer with a moderate K coverage. After CO exposure the surface was briefly heated to 485 K in UHV before the XPD data were taken. This procedure desorbs all perpendicularly adsorbed CO. None is visible in the $[1\bar{1}0]$ azimuth, and the minimum between the $\pm 32°$ peaks in the [001] azimuth is more distinct than in Fig. 5. The tilted CO is thus thermally stabilized by K. This heating would be sufficient to desorb all CO adsorbed on a clean Ni(110) surface. Our data modify the picture of CO* put forward by Whitman and Ho.[40] One can imagine the CO molecules in displaced bridge sites atop the $[1\bar{1}0]$ atomic rows tilting toward the K due to a strong, short-range electrostatic interaction. Whitman and Ho had speculated about a tilted CO* species, but thought it unlikely because the tilt would cause a weakening of the C-O stretch intensity in HREELS due to a smaller normal component of the dynamic dipole moment.

A recent LEED study of K adsorption on Ni(110) (Ref. 47) complicates the picture somewhat. The data are interpreted as a K-induced surface reconstruction of the missing-row type for $\Theta_K < 0.35$. A similar reconstruction had earlier been seen for K on Ag(110),[48] for which the missing-row structure has been confirmed by a medium-energy ion-shadowing and blocking investigation.[49] Above a K coverage of 0.35 a different LEED pattern is seen, which is thought to be from an adsorbate layer on an *unreconstructed* substrate. The model originally proposed by Gerlach and Rhodin[9] of K adsorbed in the atomic troughs along $[1\bar{1}0]$ is retained, but the K adsorption sites for $\Theta_K < 0.35$ are now at the positions of the missing-row Ni atoms. A second possible model for the CO* adsorption geometry is suggested by the missing-row reconstruction, which exposes "microfacets" having (111) orientation on the sides of the atomic troughs. The CO molecules might be displaced from the on-top adsorption sites on the rows due to an attractive interaction with K. Once on the (111) microfacet, the bonding geometry would be perpendicular [as, e.g., on Pt(111) (Refs. 10 and 37)]. These microfacets are oriented (in the ideal case, i.e., no relaxation) 35° to the surface normal—an inward relaxation of the outer atomic layer would reduce this value somewhat—so that XPD would observe the CO as being tilted, relative to the macroscopic surface, in close agreement with our measured tilt angle. Above $\Theta_K = 0.35$, where the reconstruction is lifted, the adsorption site for CO might revert to the on-top site on the $[1\bar{1}0]$ atomic row. Of course, the XPD results alone cannot fully determine the adsorption site. However, our observation of a reduced sticking coefficient and a change in tilt angle for $\Theta_K > 0.35$ are, at least, circumstantial evidence for a connection between a change in adsorption site and the change in surface reconstruction. The idea of CO adsorbed perpendicular to a facet which is vicinal to the macroscopic surface is not new. Studies of CO adsorption on Pt(533) with NEXAFS have found evidence for CO adsorbed perpendicular to the (111) microfacets on this surface.[50]

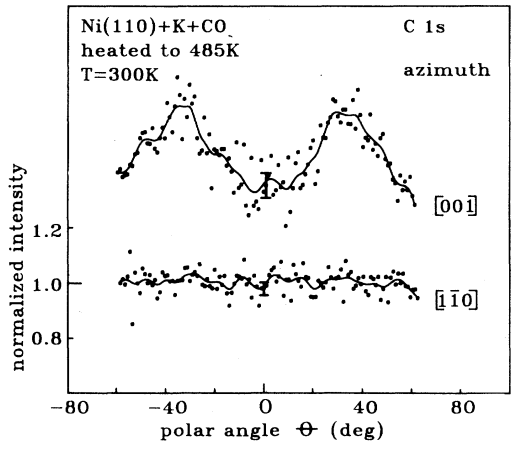

FIG. 7. Effect of briefly heating a coadsorbed layer to 485 K in UHV. Normalized C 1*s* XPD scans in both measurement azimuths are shown. The K coverage was 0.16 for the [001] azimuth and 0.19 for the $[1\bar{1}0]$ azimuth. The initial CO exposure was 3 L for both.

In comparing the results for coadsorption at 300 K of K and CO with those for CO alone at 120 K on Ni(110), we see that the two kinds of tilted CO observed have a quite similar structure: moderate polar-angle tilts ($\leq 32°$) directed along [001] and $[00\bar{1}]$ azimuths. This is in spite of the quite different origins of the tilt on clean and K-covered surfaces. CO on clean Ni(110) tilts because of a repulsive CO-CO interaction which only occurs at high coverages. Tilted CO in this case is *less* thermally stable than perpendicular CO, having a TDS peak shifted by 90 K to lower temperature.[14] On the other hand, the K-induced tilted CO observed at room temperature is due to the short-range K-CO attractive interaction. This tilted CO species is thermally more stable than the perpendicular CO, and it is observable at various CO and K coverages (in fact, at all the CO and K coverages we studied). The presence of tilted CO on clean and K-covered surfaces seems to imply that the substrate structure plays a determining role in this system, as well as adsorbate-adsorbate interaction. The change in the CO adsorption geometry on Ni(110)+K that occurs at around the K coverage at which a surface reconstruction is lifted also supports this idea.

V. SUMMARY

Our results have clearly established the existence of alkali-metal-induced CO tilting in contrast to the previous studies of this effect which were either indirect or found tilting only for very special conditions of adsorbate coverage and temperature. While the K-related, tilted CO is thermally stabilized, the deeper question of how much of this effect is attributable to the tilt itself remains open. Thermal stabilization and weakened C—O bonds are seen even in systems proven to have vertically adsorbed CO.[10,37,39] Model calculations of the relative strengths of the various kinds of CO–alkali-metal interactions would be necessary to shed light on this issue.

Regarding the growth mechanisms of the $\pm 21°$ tilted

CO species on Ni(110) at 120 K, we find that an island growth model is most probable. A mixture of perpendicular and tilted CO is present at intermediate CO coverages from about 0.40 to 0.80. Below this CO coverage range only perpendicular CO is seen, above it mostly tilted. No evidence is found for a dependence of the tilt angle on CO coverage. These coverage ranges and the coexistence behavior of tilted and perpendicular CO agree with recent LEED measurements.[14]

This study has also shown the utility of XPD in precisely determining adsorbate structure, even for relatively complicated coadsorption systems having a mixture of species with different adsorption geometries. The technique's capabilities are comparable to those of ESDIAD in this regard, but XPD measurements are not hindered by complications typical for ESDIAD, such as varying ionization cross sections, reneutralization processes leading to loss of signal, and image-potential effects. An advantage of ESDIAD compared to XPD is the speed of measurement, but this could be improved in XPD by employing more efficient multichannel detection in the electron-energy analyzer or by use of intense synchrotron radiation or rotating-anode x-ray excitation sources.

ACKNOWLEDGMENTS

We have profited from stimulating and helpful discussions with our colleagues U. Breuer, K. Dückers, G. Pirug, and K. C. Prince. We are also grateful to M. Neumann for discussing his group's XPD results with us prior to publication.

*Present address: 2. Physikalisches Institut, Rheinisch-Westfälische Technische Hochschule Aachen, Templergraben 55, D-5100 Aachen, Federal Republic of Germany.

[1]R. J. Smith, J. Anderson, and G. J. Lapeyre, Phys. Rev. Lett. **37**, 1081 (1976); C. L. Allyn, T. Gustafsson, and E. W. Plummer, Chem. Phys. Lett. **47**, 127 (1977).

[2]J. Stöhr and R. Jaeger, Phys. Rev. B **26**, 4111 (1982); J. Haase, Appl. Phys. A **38**, 181 (1985).

[3]C. S. Fadley, Prog. Surf. Sci. **16**, 275 (1984).

[4]C. S. Fadley, in *Core-Level Spectroscopy in Condensed Systems*, edited by J. Kanamor and A. Kotani (Springer, Berlin, 1988), p. 236.

[5]W. E. Egelhoff, Jr., Phys. Rev. Lett. **59**, 559 (1987).

[6]T. E. Madey, J. Vac. Sci. Technol. A **4**, 257 (1986).

[7]D. A. Wesner, F. P. Coenen, and H. P. Bonzel, Phys. Rev. Lett. **60**, 1045 (1988).

[8]D. A. Wesner, F. P. Coenen, and H. P. Bonzel, Surf. Sci. **199**, L419 (1988).

[9]R. L. Gerlach and T. N. Rhodin, Surf. Sci. **17**, 32 (1969).

[10]D. A. Wesner, F. P. Coenen, and H. P. Bonzel, Phys. Rev. B **33**, 8837 (1986).

[11]H. P. Bonzel, Surf. Sci. Rep. **8**, 43 (1987).

[12]H. H. Madden, J. Küppers, and G. Ertl, J. Chem. Phys. **58**, 3401 (1973); T. N. Taylor and P. J. Estrup, J. Vac. Sci. Technol. **10**, 26 (1973).

[13]B. J. Bandy, M. A. Chesters, P. Hollins, J. Pritchard, and N. Sheppard, J. Mol. Struct. **80**, 203 (1980).

[14]R. J. Behm, G. Ertl, and V. Penka, Surf. Sci. **160**, 387 (1985).

[15]B. A. Gurney and W. Ho, J. Vac. Sci. Technol. A **3**, 1541 (1985).

[16]H. Kuhlenbeck, M. Neumann, and H.-J. Freund, Surf. Sci. **173**, 194 (1986).

[17]M. D. Alvey, M. J. Dresser, and J. T. Yates, Jr., Surf. Sci. **165**, 447 (1986).

[18]W. Riedl and D. Menzel, Surf. Sci. **163**, 39 (1985).

[19]C. W. Bauschlicher, Jr., Chem. Phys. Lett. **115**, 535 (1985).

[20]L.-G. Petersson, S. Kono, N. F. T. Hall, C. S. Fadley, and J. B. Pendry, Phys. Rev. Lett. **42**, 1545 (1979).

[21]K. C. Prince, E. Holub-Krappe, K. Horn, and D. P. Woodruff, Phys. Rev. B **32**, 4249 (1985).

[22]D. A. Wesner, F. P. Coenen, and H. P. Bonzel, J. Vac. Sci. Technol. A **5**, 927 (1987).

[23]K. A. Thompson and C. S. Fadley, J. Electron Spectrosc. Relat. Phenom. **33**, 29 (1984).

[24]N. V. Richardson and A. M. Bradshaw, Surf. Sci. **88**, 255 (1979).

[25]M. Fink and J. Ingram, At. Data **4**, 129 (1972).

[26]H. C. Poon, D. Snider, and S. Y. Tong, Phys. Rev. B **33**, 2198 (1986); M. Sagurton, E. L. Bullock, R. Saiki, A. Kaduwela, C. R. Brundle, C. S. Fadley, and J. J. Rehr, *ibid.* **33**, 2207 (1986).

[27]S. K. Saha and B. C. Khanra, Phys. Rev. B **31**, 5521 (1985).

[28]F. M. Hoffmann and R. A. de Paola, Phys. Rev. Lett. **52**, 1697 (1984); R. A. de Paola, J. Hrbek, and F. M. Hoffmann, J. Chem. Phys. **82**, 2484 (1985).

[29]T. E. Madey and C. Benndorf, Surf. Sci. **164**, 602 (1985).

[30]M. D. Alvey, A.-M. Lanzillotto, and J. T. Yates, Jr., Surf. Sci. **177**, 278 (1986).

[31]D. Heskett, E. W. Plummer, R. A. de Paola, and W. Eberhardt, Phys. Rev. B **33**, 5171 (1986).

[32]D. Heskett, I. Strathy, E. W. Plummer, and R. A. de Paola, Phys. Rev. B **32**, 6222 (1985).

[33]W. Wurth, J. J. Weimer, E. Hudeczek, and E. Umbach, Surf. Sci. **173**, L619 (1986).

[34]F. P. Netzer, D. L. Doering, and T. E. Madey, Surf. Sci. **143**, 1363 (1984).

[35]D. Lackey, M. Surman, S. Jacobs, D. Grider, and D. A. King, Surf. Sci. **152/153**, 513 (1985).

[36]J. Arias, J. Lee, J. Dunaway, R. M. Martin, and H. Metiu, Surf. Sci. **159**, L433 (1985).

[37]F. Sette, J. Stöhr, E. B. Kollin, D. J. Dwyer, J. L. Gland, J. L. Robbins, and A. L. Johnson, Phys. Rev. Lett. **54**, 935 (1985).

[38]D. A. Wesner, G. Pirug, F. P. Coenen, and H. P. Bonzel, Surf. Sci. **178**, 608 (1986).

[39]G. Pirug and H. P. Bonzel, Surf. Sci. **199**, 371 (1988).

[40]L. J. Whitman and W. Ho, J. Chem. Phys. **83**, 4808 (1985).

[41]L. H. Dubois, B. R. Zegarski, and H. S. Luftman, J. Chem. Phys. **87**, 1367 (1987).

[42]D. A. Wesner, F. P. Coenen, and H. P. Bonzel, Langmuir **1**, 478 (1985).

[43]D. A. Wesner, G. Linden, and H. P. Bonzel, Appl. Surf. Sci. **26**, 335 (1986).

[44]J. J. Weimer and E. Umbach, Phys. Rev. B **30**, 4863 (1984); J. J. Weimer, E. Umbach, and D. Menzel, Surf. Sci. **159**, 83 (1985).

[45]M. Kiskinova, A. Szabo, and J. T. Yates, Jr., Phys. Rev. Lett. **61**, 2875 (1988).

[46]G. Brodén, G. Gafner, and H. P. Bonzel, Surf. Sci. **84**, 295 (1979); J. Benziger and R. J. Madix, *ibid.* **94**, 119 (1980); M. P.

Kiskinova, G. Pirug, and H. P. Bonzel, *ibid.* **133**, 321 (1983); C. Somerton, C. F. McConville, D. P. Woodruff, D. E. Grider, and N. V. Richardson, *ibid.* **138**, 31 (1984); J. Lee, J. Arias, C. P. Hanrahan, R. M. Martin, and H. Metiu, J. Chem. Phys. **82**, 485 (1985).

[47]D. K. Flynn, K. D. Jamison, P. A. Thiel, G. Ertl, and R. J. Behm, J. Vac. Sci. Technol. A **5**, 794 (1987); Phys. Rev. B **36**, 9267 (1987).

[48]B. E. Hayden, K. C. Prince, P. J. Davie, G. Paolucci, and A. M. Bradshaw, Solid State Commun. **48**, 325 (1983).

[49]J. W. M. Frenken, R. L. Krans, and J. F. van der Veen, Phys. Rev. Lett. **59**, 2307 (1987).

[50]J. S. Somers, Th. Lindner, M. Surman, A. M. Bradshaw, G. P. Williams, C. F. McConville, and D. P. Woodruff, Surf. Sci. **183**, 576 (1987).